Ring Filters and Small-Sized Wideband Ring Filters

Hee-Ran Ahn · Noh-Hoon Myung

Abstract

A ring filter is proposed as a wide-banded filter. It consists of a ring and two short stubs, which are connected at 90° and 270° points of the ring. Since the termination impedance at 90° and 270° points of the ring and the characteristic impedance of the short stub have an effect on designing of it, the relation between them and bandwidths has been studied. Based on the study, two types of small-sized wideband CVT(constant VSWR-type impedance transformer)- and CCT(constant conductance-type impedance transformer)-ring filters are introduced, designed, simulated and one of two, a CCT-ring filter, is tested. The circumference of the ring can be reduced theoretically up to 60° and two of many cases having about 300° circumferences are simulated. The simulated results show more than 100 % fractional bandwidth, which can be obtained with more than 5 stages in conventional filter-design techniques. To test the designed CCT-ring filter, it has been fabricated in microstrip technology and the measured results show good agreement with the simulated ones, having more than 100 % fractional bandwidth.

Key words : Ring Filters, Small-Sized Wideband Ring Filters, Small-Sized Impedance Transformers(CCVTs and CCTs).

Ⅰ. Introduction

It is well known that ring resonators have low radiation loss, high Q factors and two orthogonal resonant modes. Because of these special properties, ring resonators have widely been used for the measurements[1],[2], band-pass filters and duplexers[3]. Microstrip open- and closed-ring resonators were intensively discussed[4],[5] and mixers, oscillators and tuning filters have been realized based on circuit theory concepts[6]. However, these circuits suffer from high insertion loss due to the gap discontinuities and inaccurate analyses of the gap capacitances, which can not be neglected.

The band-pass design techniques have been discussed based on quarter wave impedance transformers and the design bandwidths may range from narrow band on up to such wide bandwidths, their fractional bandwidths greater than 135 %[7]. In this paper, wideband, small-sized ring filters are introduced, designed and measured. The ring filter was for the first time introduced as a wideband 180° phase shifter[8] where feeding lines are directly coupled to a ring to reinforce high insertion loss caused by gaps in conventional ring-based circuits, and two short stubs are connected at 90° and 270° points of the ring to reject DC and even-multiples of a design center frequency. Since the termination impedance where each short-stub is connected has an effect on designing of the ring filters, it is defined as a hypothetical port and the relations between bandwidths and the termination impedance, characteristic impedance of the short stub are studied. Based on the study, optimal values of them are selected for a wideband ring filter. To reduce the size of ring filters, CVTs and CCTs[9] are good candidates. While conventional quarter-wave impedance transformers have only 90° phase shift, the CVTs and CCTs have arbitrary phase responses less than 90°, which can be used for various applications. These distinctive characteristics make the ring filters small-sized by replacing four transmission line sections with the CVTs and CCTs, and the two types of small-sized ring filters are named CVT- and CCT-ring filters. The circumference of the ring can be reduced up to 60° and two cases having about 300° circumferences are simulated and compared. The simulated results show more than 100 % fractional bandwidths with return losses less than - 15 dB, which can be obtained with more than 5 stages in conventional filter design techniques. To verify the performances, a CCT ring filter has been measured and the measured results show good agreements with the simulated ones.

Manuscript received August 7, 2003 ; revised September 17, 2003.

Division of Electrical Engineering, Dept. of EECS, KAIST, Korea.

Ⅱ. Ring Filters

A ring filter is depicted in Fig. 1(a) and its up-filter in Fig. 1(b). It is terminated in Z_1 and Z_2, and consists of a ring and two short stubs. The two short-stubs are located at 90° and 270° points of the ring and the point where each short stub is connected may be considered as a hypothetical port whose termination impedance is Z_h. The Z_h is needed to design the ring filters and may arbitrarily be chosen when $Z_1=Z_2$, and $Z_h=(Z_1+Z_2)/2$ or $\sqrt{Z_1Z_2}/2$ in the case of $Z_1\neq Z_2$. The length of four transmission-line sections forming a ring is equally l and their characteristic impedances are Z_{ca}, Z_{cb}, Z_{cc} and Z_{cd}. If the two short stubs do not exist in Fig. 1(a), all the power excited at port ① will be delivered to port ② at all frequencies, and perfect matching occurs at multiples of the design center frequency. Therefore, each stub is necessary to reject the power at the even multiples of the design center frequency and to achieve filter characteristics as a resonator. To reinforce high insertion loss caused by gaps in conventional ring-based circuits, two feeding lines are directly coupled to the ring. Since lengths of the two short stubs are about 90°, the power excited at port ① is divided depending on the power division ratio of d_1 to d_2 indicated in Fig. 1(a), and the divided power is combined at port ②[11],[12]. Thus, it can be understood in such way the two filters, "up-filter" and "down-filter" shown in Fig. 1(a), are connected in parallel and the termination impedances of the up-filter may be derived as explained in Fig. 1(b)[11]. Z_s, l_{us} and l_{ds} are characteristic impedance, lengths of the two short stubs of up- and down-filters, respectively.

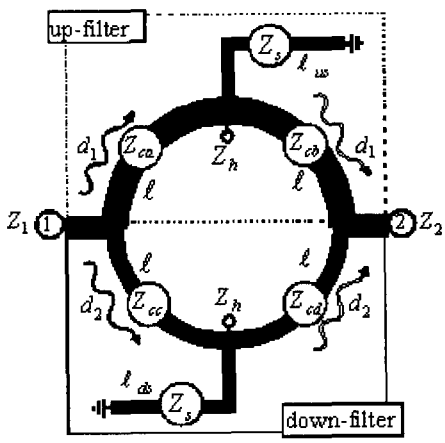

(a)

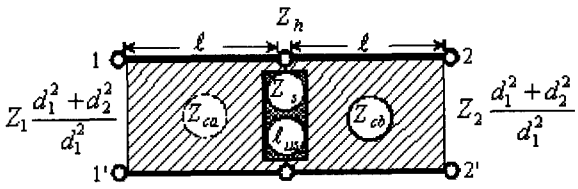

(b)

Fig. 1. Ring filter.
(a) Ring filter, (b) Up-filter

The *ABCD* parameters of the up-filter in Fig. 1(b) are

$$A_{up}=\cosh^2 rl+\frac{Z_{ca}}{2Z_s}\sinh 2rl\coth rl_{us}+\frac{Z_{ca}}{Z_{cb}}\sinh^2 r\lambda$$

$$B_{up}=\frac{Z_{ca}+Z_{cb}}{2}\sinh 2rl+\frac{Z_{ca}Z_{cb}}{Z_s}\sinh^2 rl\coth rl_{us},$$

$$C_{up}=\frac{\sinh 2rl}{2Z_{ca}}+\frac{1}{Z_s}\cosh^2 rl\coth rl_{us}+\frac{\sinh 2rl}{2Z_{cb}},$$

$$D_{up}=\frac{Z_{cb}\sinh^2 rl}{Z_{ca}}+\frac{Z_{cb}}{2Z_s}\coth rl_{us}\sinh 2rl+\cosh^2 rl, \quad (1)$$

Where,

$r=\alpha+j\beta$ (α and β : attenuation and phase constants),

$$Z_{ca}=\sqrt{Z_1Z_h\frac{d_1^2+d_1^2}{d_1^2}},$$

$$Z_{cb}=\sqrt{Z_2Z_h\frac{d_1^2+d_2^2}{d_1^2}}. \quad (2)$$

In the same way, those of the down-filter are

$$A_{up}=\cosh^2 rl+\frac{Z_{cc}}{2Z_s}\sinh 2rl\coth rl_{ds}+\frac{Z_{cc}}{Z_{cb}}\sinh^2 rl$$

$$B_{do}=\frac{Z_{cc}+Z_{cb}}{2}\sinh 2rl+\frac{Z_{cc}Z_{cb}}{Z_s}\sinh^2 rl\coth rl_{ds},$$

$$C_{do}=\frac{\sinh 2rl}{2Z_{cc}}+\frac{1}{Z_s}\cosh^2 rl\coth rl_{ds}+\frac{\sinh 2rl}{2Z_{cd}},$$

$$D_{do}=\frac{Z_{cb}\sinh^2 rl}{Z_{cc}}+\frac{Z_{cd}}{2Z_s}\coth rl_{ds}\sinh 2rl+\cosh^2 rl, \quad (3)$$

Where,

$$Z_{cc}=\sqrt{Z_1Z_h\frac{d_1^2+d_2^2}{d_2^2}},$$

$$Z_{cb}=\sqrt{Z_2Z_h\frac{d_1^2+d_2^2}{d_2^2}}. \quad (4)$$

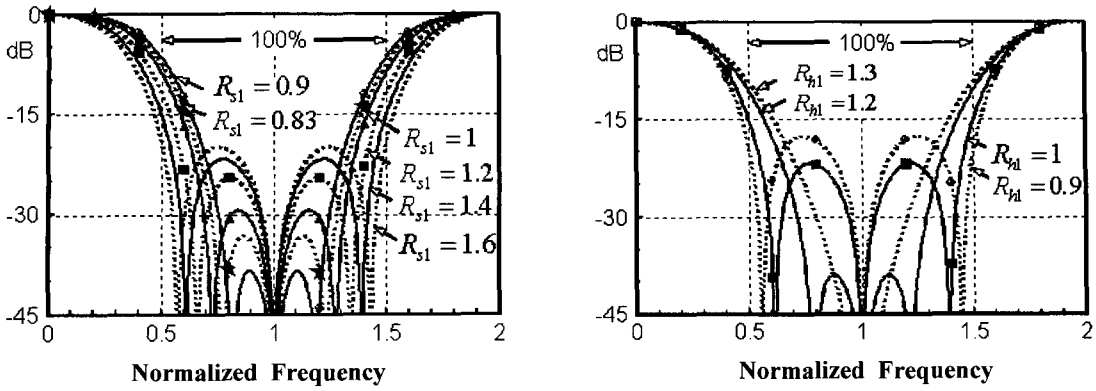

Fig. 2. Calculated reflection coefficients.
(a) Reflection coefficients depending on R_{s1} with $Z_1=Z_2=Z_h$
(b) Those of R_{h1} with $R_{s1}=1.4$

Using a relation between the *ABCD* and admittance parameters, the *Y*-parameters contributed by port ① and ② may be derived as

$$Y_{11}=\frac{D_{up}}{B_{up}}+\frac{D_{do}}{Bo_{do}},$$

$$Y_{12}=Y_{21}=-\left(\frac{1}{B_{up}}+\frac{1}{B_{do}}\right),$$

$$Y_{22}=\frac{A_{up}}{B_{up}}+\frac{A_{do}}{Bo_{do}}, \tag{5}$$

If port ② is terminated in Z_2 as shown in Fig. 1(a), the reflection coefficient at port ①

Γ is

$$\Gamma=\frac{1-Y_{in}Z_1}{1+Y_{in}Z_1}, \tag{6}$$

where $Y_{in}=\dfrac{Y_{22}+Y_2}{Y_{11}(Y_{22}+Y_2)-Y_{12}Y_{21}}$ and $Y_2=1/Z_2$.

Based on (1)~(6), frequency responses of the reflection coefficients Γ have been calculated by a program working on a mathematical program, Matlab 6.1. For simplicity, $\alpha=0$ (lossless), no discontinuity effect, $Z_1=Z_2$, $d_1=d_2$, $\beta_0 l=\beta_0 l_{us}=\beta_0 l_{ds}=90°$ are considered where β_0 is a propagation constant at a design center frequency. Two types of calculated results are plotted in Fig. 2 where the "R_{s1}" is the ratio of Z_s to Z_1 and "R_{h1}" that of Z_h to Z_1 in Fig. 1(a). Fig. 2(a) show those depending on different values of in the case of $Z_1=Z_2=Z_h$. The calculated results in Fig. 2(a) indicate higher values of Z_s have wider bandwidths and that fractional bandwidth is about 100 % with $R_{s1}=1.4$, when its fractional bandwidth is defined as a frequency range where Γ is less than −15 dB. Those for various values of R_{h1} are plotted in Fig. 2(b), and all are the cases of $R_{s1}=1.4$, or $Z_s=1.4Z_1$. From those in Fig. 2(b), it may be known that the bandwidths become smaller as the R_{h1} increases. Up to $R_{h1}=1.2$ three poles exist, which is a prime cause of the wideband characteristics of the ring filters. However, it does not appear with $R_{h1}=1.3$. Therefore, if the Z_s and Z_h are properly chosen, ring filters with the fractional bandwidth greater than 100 % may be designed.

The relation between fractional bandwidth ω_f and ripple VSWR (voltage standing wave ratio) is expressed as VSWR=1+(2 ω_f)^2 in conventional filter design[7] and plotted in Fig. 3. It expresses, as the ω_f increases,

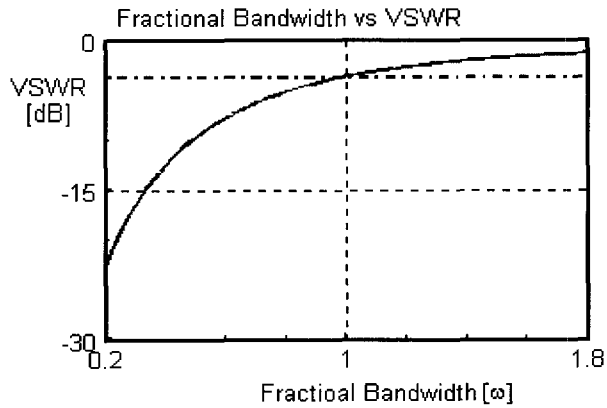

Fig. 3. A relation between fractional bandwidth and VSWR ripple.

match may not easily be achieved and the VSWR is less than −5 dB when ω_f = 100 %, which demonstrates that the ring filters definitely have advantages in terms of wideband filter design.

Ⅲ. Small-Sized Wideband Ring Filters

When $\beta_0 l$= 90°, the transmission line sections with Z_{ca}, Z_{cb}, Z_{cc} and Z_{cd} in Fig. 1(a) are all impedance transformers to transform a real impedance into another one. To reduce the size of them, two types of small-sized impedance transformers, CVTs and CCTs[9] are good candidates. Fig. 4 show three different impedance transformers to transform a real impedance (*IR*) into another real one(unity) where the CVT and CCT are in Fig. 4(a) and (b), respectively, whereas a conventional quarter-wave one in Fig. 4(c). Thus, the *IR* becomes an impedance-transformation ratio. All the values of z_a, z_b, z_c and z_d together with Θ_a, Θ_b, Θ_c and Θ_d in Fig. 4(a) and (b) may be calculated on a Smith chart and how to derive is explained in [9].

Phase responses of S_{12} of CVT and CCT in Fig. 4(a) and (b) have been calculated, depending on the *IR*. The calculation has been carried out under ideal conditions (lossless and no discontinuity effect) based on the formulas derived in Appendix[13]. The calculated results of the CVTs are plotted in Fig. 5(a), whereas those of the CCTs in Fig. 5(b). From the results in Fig. 5, the

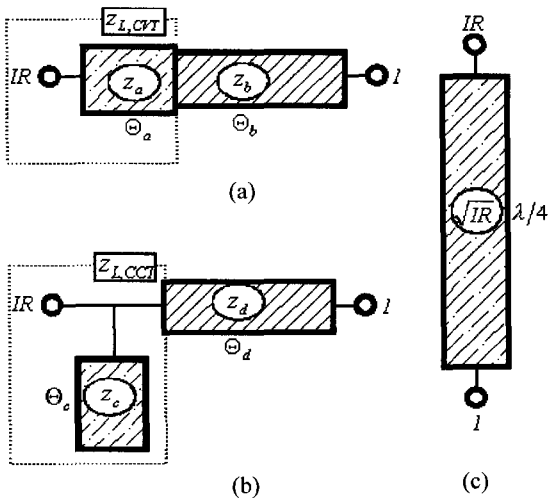

Fig. 4. Three types of impedance transformers.
(a) CVT
(b) CCT
(c) A conventional quarter-wave impedance transformer

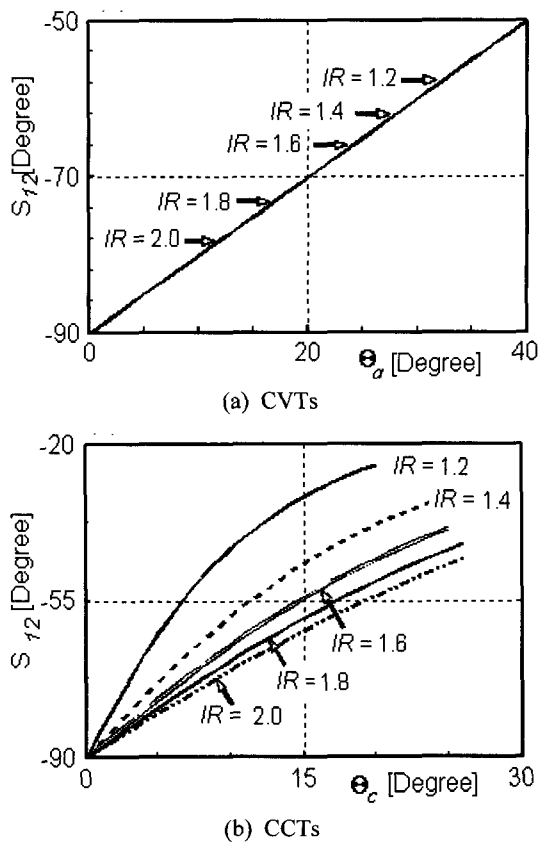

Fig. 5. The phase responses of S_{12}.

CVTs and CCTs are all quarter-wave impedance transformers with Θ_a= Θ_c=0° and their phases of S_{21} are equally 90°. As Θ_a becomes longer, those of S_{21} are almost linear independently on the *IR* and arbitrary phase responses less than 90° may be obtained. With the value of Θ_c increasing in Fig. 5(b), arbitrary phases of S_{21} can also be achieved up to around 30°. This fact of arbitrariness is quite distinct from conventional quarter-wave ones, and the CVTs and CCTs may be used for various applications.

The input impedances looking into the load *IR* in Fig. 4(a) and (b), $z_{L,CVT}$ and $z_{L,CCT}$, are given as

$$z_{L,CVT} = z_a \frac{IR + jz_a \tan\Theta_a}{z_a + jIR\tan\Theta_a},$$

$$z_{L,CCT} = \frac{z_c IR}{jIR tan\Theta_c + z_c}. \quad (7)$$

(7) expresses both of real and imaginary parts of $z_{L,CVT}$ are changed at the same time with changes in z_a but that $z_{L,CCT}$ is not varied with the z_c. Thus, z_a must be unity as demonstrated in the previous work[9] but z_c

can have other values including the unity.

To reduce the size of the ring filters, a ring filter as shown in Fig. 1(a) is needed and the calculated results in Fig. 2 express that it has wider bandwidths with higher values of Z_s and lower ones of Z_h. Therefore, optimal Z_h and Z_s may be used for small-sized wideband ring filters. For this, one with $Z_1=Z_2=Z_h=50$ Ω and $Z_s=85$ Ω can be chosen and its impedance-transformation ratio IR is 2 in the case of $d_1=d_2$, referring to (2), (4) and Fig. 1(b). Therefore, the four transmission line sections in Fig. 1(a) can be replaced with the CVTs and CCTs with $IR=2$. The resulting configurations are illustrated in Fig. 6 and named CVT- and CCT-ring filters in Fig. 6(a) and (b), respectively.

All the data needed for the design of three ring filters including CVT- and CCT- ring filters are given in Table 1. As explained in (7), $z_c=30$ Ω is chosen for better open-stub performance and simulated results of them are plotted in Fig. 7 where "Con-Ring" is the ring filter shown in Fig. 1 and "CVT-Ring" and "CCT-Ring" are the CVT- and CCT-ring filters in Fig. 6 (a) and (b), respectively. Frequency responses of insertion loss are plotted in Fig. 7(a) and reflection coefficients in Fig. 7(b). They are also summarized in Table 1. The simulated results show about same performances even if the length of each transmission line and the circuit configurations are different from each other. As given in Table 1, all the three ring filters have more than 100 % fractional bandwidth with less than 0.1 dB attenuation and less than −15 dB reflection coefficients.

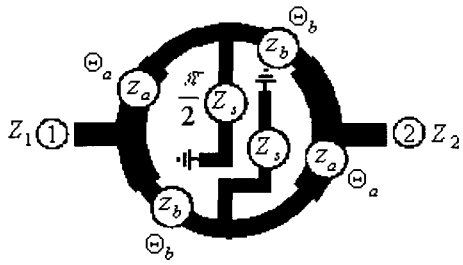

(a) A CVT- ring filter

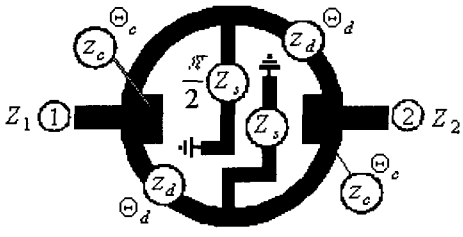

(b) A CCT- ring filter

Fig. 6. Small-sized wideband ring filters.

Table 1. Design data and simulated results for a ring filter, CVT- and CCT-ring filters.

Ring filter	CVT-Ring filter	CCT-Ring filter
$Z_1=Z_2=50$ Ω $Z_s=85$ Ω	$Z_1=Z_2=50$ Ω $Z_s=85$ Ω	$Z_1=Z_2=50$ Ω $Z_s=85$ Ω
$Z_{ca}=Z_{ch}=Z_{cc}$ $=Z_{cd}=70.71$ Ω	$z_a=50$ Ω $\Theta_a=10°$ $Z_h=72.4$ Ω $\Theta_b=68.7°$	$z_c=30$ Ω $\Theta_c=5°$ $z_d=71.8$ Ω $\Theta_d=75.89°$
Bandwidth with insertion loss less than −0.1 dB		
0.47～1.53 GHz	0.48～1.52 GHz	0.48～1.52 GHz
Bandwidth with return loss less than −15 dB		
0.46～1.54 GHz	0.43～1.57 GHz	0.44～1.56 GHz

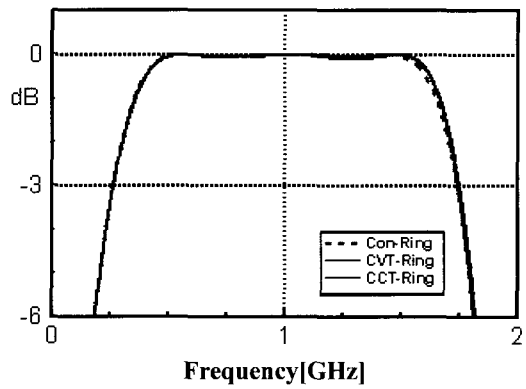

(a) Insertion losses

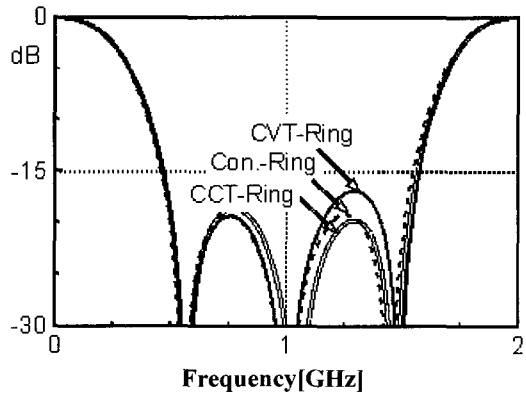

(b) Return losses(reflection coefficients)

Fig. 7. Simulated results of three ring filters.

Based on the design data, the CCT-ring filter has been fabricated on a substrate of ($\varepsilon_r=2.88$, $h=508\,\mu$m, $\tan\delta=0.0064$ at 3 GHz) in microstrip technology. The

Table 2. Fabrication data for a CCT-ring filter.

$Z_1=Z_2=50\ \Omega$	
$Z_s=85\ \Omega$ $\Theta_s=90°$	$W=509\ \mu m$ $lus=lds=16810\ \mu m$
$z_c=30\ \Omega$ $\Theta_c=5°$	$W=2703\ \mu m$ $l=880.6\ \mu m$
$z_d=71.8\ \Omega$ $\Theta_d=75.89°$	$W=711.5\ \mu m$ $l=14035\ \mu m$

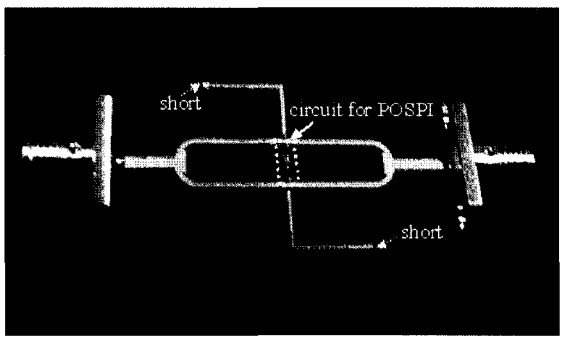

(a) Layout for the CCT-ring filter

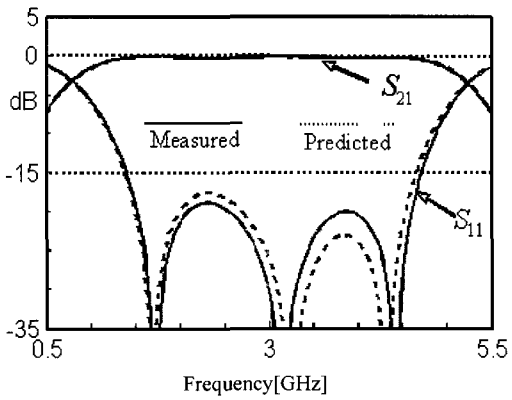

(b) Measured and predicted ressults

Fig. 8. A CCT-ring filter for the measurements.

fabrication data are given in Table 2. and it has been designed at the center frequency of 3 GHz. A photo of the CCT-ring filter is given in Fig. 8(a) and the measured and predicted results are compared in Fig. 8(b). In practical case, the phases of S_{21} of the up- and down filters are not always same because the two short stubs could not be realized equally. That causes a sudden phase inversion and any circuit between the two Z_h ports in Fig. 1 is needed to prevent it. The circuit for POSPI(prevent of sudden phase-inversion) shown in Fig. 8(a) is one of them and consists of two resistors. The resistance could be several ohms and two chip resistors with a 10 Ω are used for the sufficient distance between the two transmission lines. The predicted results in Fig. 8(b) have been carried out using a EM-simulator, Empire[1] based on FDTD(finite difference time domain).

[1]Empire, a E-M simulator produced by IMST, Kamp-Lintfort, Germany, 2001.

The deviation at the edge of the pass-band between the measured and predicted ones is due to the stray capacitance and inductance caused by soldering the two resistors on the transmission lines. Except that points, the measured results agree well with the predicted ones.

Ⅳ. Conclusions

A Ring filter is suggested as a wide-banded filter. It consists of a ring and two short stubs connected at 90° and 270° points of the ring. The termination impedance of the position where the short stubs are connected and the characteristic impedance of the short stub are related with the bandwidths of the ring filter, optimal values of them are needed for small-sized wideband ring filters. Based on the ring filter selected, small-sized CVT- and CCT-ring filter are designed and a CCT-ring filter is tested. Since the phase shifts of the CVT- and CCT-ring filters are arbitrary, they can be used for various devices in microwave applications. The measured bandwidths of the small-sized CVT- and CCT-ring filters show more than 100 %, which can be designed with more than 5 stages in conventional filter design technique.

This work is supported by a BK21 program at KAIST, and in Part by the KOSEF(Korea Science & Engineering Foundation) through the MICROS at KAIST and EMERC(Electromagnetic Environment Research Center) at chungnam National Univ.

References

[1] I. Wolff, N. Knoppik, "Microstrip ring resonator and dispersion measurement on microstrip lines", *Electronic. Lett.*, vol. 7, no. 26, pp. 779-781, Dec. 1971.

[2] I. Wolff, "Microstrip bandpass filter degenerate modes of a microstrip ring resonator", *Electronic. Lett.*, vol. 8, no. 12, pp. 302-303, Jun. 1972.

[3] H. Yabuki, M. Sagawa, M. Matsuo and M. Makimoto, "Stripline dual-mode ring resonators and their application to microwave devices", *IEEE Trans. Microwave Theory Tech.*, vol. 44, pp. 723-729, May 1996.

[4] I. Wolff, V. Tripathi, "The microstrip open-ring resonator", *IEEE Trans. Microwave Theory Tech.*, vol. MTT-32, pp. 102-107, Jan. 1984.

[5] V. Tripathi, I. Wolff, "Perturbation analysis and design equations for open- and closed-ring microstrip resonators", *IEEE Trans. Microwave Theory Tech.*, vol. MTT-32, pp. 409-410, Apr. 1984.

[6] K. Chang, S. Martine M. Fuchen and J. L. Kline, "On the study of microstrip ring and varactor-tunned ring circuits", *IEEE Trans. Microwave Theory Tech.*, vol. MTT-35, pp. 1288-1295, Dec. 1987.

[7] G. Matthaei, L. Young and E. M. T. Jones, *Microwave Filters, Impedance-Matching Networks, and Coupling Structures*, Artech House Books. Dedham, MA, pp. 562, pp. 521, 1980.

[8] H.-R. Ahn, Ingo Wolff, "Novel ring filter as a wide-band 180° transmission-line", in *1999 European Microwave Conference Proceedings*, Munich (Germany), vol. III, pp. 95-98, Oct. 1999.

[9] H.-R. Ahn, I. Wolff, "General design equations, small-sized impedance transformers, and their applications to small-sized three-port 3-dB power dividers", *IEEE Trans. Microwave Theory Tech,* vol. 49, pp. 1277-1288, July 2001.

[10] H.-R. Ahn, I.-S. Chang and S.-W. Yun, "Miniaturized 3-dB ring hybrid terminated by arbitrary impedances", *IEEE Trans. Microwave Theory Tech.*, vol. 42, pp. 2216-2241, Dec. 1994.

[11] H.-R. Ahn, I. Wolff, "Arbitrary termination impedances, arbitrary power division and small-sized ring hybrids", *IEEE Trans. Microwave Theory Tech.*, vol. 44, pp. 2241-2247, Dec. 1997.

[12] H.-R. Ahn, I. Wolff, "Three-port 3-dB power divider terminated by different impedances and its application to MMIC's", *IEEE Trans. Microwave Theory Tech.*, vol. 47, pp. 786-794, June 1999.

[13] H.-R. Ahn, I. Wolff, "Asymmetric ring hybrid phase-shifters and attenuators", *IEEE Trans. Microwave Theory Tech.*, vol. 50, pp. 1146-1155, April 2002.

Hee-Ran Ahn

Hee-Ran Ahn received the B.S., M.S., and Ph.D. degrees in electronic engineering from Sogang University, Seoul, Korea, in 1988, 1990 and 1994, respectively. From 1991 to 1995, she was a Part-Time Lecturer at Sogang University, Seoul, Korea and a Post- Doctoral Fellow from 1996 to 1997 at Duisburg-Essen University, Duisburg, Germany. From February 1997 to 2002, she was with the Department of Electrical Engineering at Duisburg-Essen University, Duisburg, Germany where she worked for the Habilitation dealing with asymmetric passive components. She is currently with Division of Electrical Engineering, Dept. EECS at KAIST(Korea Advanced Institute Science and Technology), Daejeon, Korea as a Visiting professor. She is a Senior Member of IEEE since 1999 and in editorial board at IEEE on MTT(Microwave Theory and Technology). Her interests include high frequency and microwave circuit design, and biomedical application of microwave theory and techniques.

Noh-Hoon Myung

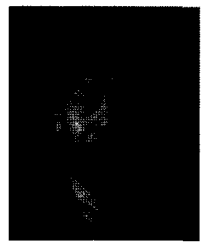

was born in Seoul, Korea, in 1953. He received the B.S. degree in electrical engineering from the Seoul National University, Korea, in 1976, and the M.S. and Ph.D. degrees from the Ohio State University, Columbus, in 1982 and 1986, respectively. He was a Research Member at the ElectroScience Laboratory, Ohio State University, for six years, working in the area of electromagnetic wave scattering and propagation before joining the EECS Dept., Korea Advanced Institute of Science and Technology(KAIST). He was also a member of the research staff of the National Highway Traffic and Safety Administration(NHTSA), Ohio, where he constructed a ground-based optical vehicle tracking system. His current research areas include wave scattering and propagation analysis, RCS(radar cross section) analysis, antenna and radar system design, mobile and satellite communications, and electromagnetic interference and electromagnetic compatibility (EMI/EMC).